The Journal of the Korean Society of Oceanography
Vol. 32, No. 3, pp. 93-102, September 1997

Effect of the Bottom Slope on the Formation of Coastal Front and Shallow-Sea Structure during Cold-Air Outbreak

HYEONG-BIN CHEONG, YOUNG-SEUP KIM AND SUNG-KEUN HONG[1]
Department of Earth Environmental Sciences, School of Marine Science and Technology, Pukyong National University, Pusan 608-737, Korea
[1]Department of Marine Production, Kunsan National University, Kunsan 573-701, Korea

Coastal circulations during the (surface condition of an) idealized cold-air outbreak are numerically investigated with two-dimensional, non-hydrostatic model in which a constant bottom-slope exists. The atmospheric forcing during a cold-air outbreak is incorporated as the surface cooling and the wind stress. When the offshore angle of the wind-stress vector, defined as the angle measured from the alongshore axis, is smaller than 45 degrees, a strong down-welling circulation develops near the coast. A sharp density front, which separates the vertically homogeneous region from the offshore stratified region, is formed near the coast and propagates offshore with time. Onshore side of the density front, small-scale circulation cells which are aligned in the direction perpendicular to the bottom begin to develop as the near-coast homogeneous region broadens. The surface cooling enhances greatly the development of the surface mixed layer by convective motions due to hydrostatic instability. The convective motions reach far below the hydrostatically unstable layer which is attached to the surface. The small-scale circulation cells are appreciably modified by the convetion cell and the density front develops far offshore compared to the case of no surface cooling. As to the effect of the bottom slope, the offshore distance of the density front increases (decreases) as the bottom slope decreases (increases), which results from the fact that the onshore volume-transport (Ekman transport) of the low-density upper seawater remains almost constant when the wind-stress is maintained constant. It is shown that the bottom slope is an essential factor for the formation of both the density front and the alongshore current when the surface cooling is the only forcing.

INTRODUCTION

Two dimensional coastal circulations in the cross-shelf section near the coast are studied numerically by authors for various conditions (e.g., Akimoto *et al.*, 1990; Allen *et al.*, 1995; Federiuk and Allen, 1995, 1996; Allen and Newberger, 1996). Through these studies, the physical factors such as wind stress, surface heating or cooling, and bottom slope emerged to be of primary importance in determining the density structure and circulation of the coastal seawater.

Akimoto *et al.* (1990) emphasized the importance of the nonhydrostatic process and the lateral buoyancy-flux to the formation of the shallow sea front by resolving the convective process in a numerical model. They showed that the gravitational convection enhances the cooling rate of the coastal seawater by about ten times compared to the hydrostatic model, when the same surface heat flux is given. However, since they used a model of constant depth, the role of bottom slope for the formation of a shallow sea front was not made clear. Feliks (1991) examined the effects of successive winter-storms (i.e., intermittent atmospheric forcing) on the development of the downwelling circulation in a deep coastal sea. He found that a downwelling zone near the coast, about 100 km wide, is formed and the isotherms decline by more than 250 m near the coast.

Coastal circulations in the presence of the realistic bottom slope were investigated by Allen *et al.* (1995), Allen and Newberger (1996) and Federiuk and Allen (1996) based on the hydrostatic model. Allen and Newberger (1996) found that the small-scale circulation (cells) develops at the bottom near the coast under the condition of surface heating and the downwelling favorable wind-stress forcing. The small-scale circulation cells propagate onshore with a typical speed of 1 km/day, which is

comparable to the offshore propagation speed of the small-scale circulation cells group. The scale of these circulations is about 1 km or less in horizontal direction and 50 m in vertical direction. In the model of Allen and Newberger, the surface heating, which tends to make a stable stratification, is considered to be an important factor that maintains the surface layer neutral stratification against the strong advection of the high-density seawater from the offshore region.

In the context of air-sea interaction during a cold-air outbreak Chao (1992) studied the coastal circulation with an atmosphere-ocean coupled model which has a horizontal scale comparable to that of the cold front in the atmosphere. He noticed that the ocean cooling should be treated as a function of the wind stress in order to estimate properly its effect on the coastal circulation. Since his main concern was the large-scale behavior of the atmosphere and ocean coastal circulations near the coast were not presented in detail.

The purpose of this study is to investigate the two-dimensional (cross-shelf) coastal circulations during a cold-air outbreak which are primarily driven by the wind stress in the presence of *the bottom slope*. We use the Boussinesq model which is identical to that used by Cheong and Han (1997) incorporating a typical winter condition of the East Sea. Though the bottom slope of the coastal sea is generally very small, its effects on circulations are so great, as suggested by Allen *et al.* (1995) etc., because the depth variation with the offshore distance near the coast is large. In the East Sea, both the wind stress and surface cooling reaches the maximum in winter because the wind over the sea is strongest and temperature difference between the air and the sea is greatest of the year (Na, 1988; Kang *et al.*, 1994). The magnitude and direction of wind-stress vector over the East Sea in January is about 2.5 dyne/cm^2 and of southeast direction, reflecting cold-air outflow from the northwest (Kang *et al.*, 1994). However, the wind stress vector over the same area in February, calculated by Na (1988), directs nearly eastward and its magnitude is one order smaller than that in January calculated by Kang *et al.* (1994). Such a great difference even in the same season may result from using different dataset and estimating method (e.g., see Kim and Kimura, 1995). Estimation by Kang *et al.* (1994) indicates that the time-mean net heat flux (i.e., latent heat flux plus sensible heat flux) to the atmosphere in January ranges from 100 to 400 W/m^2.

The experimental situation in this study shares some common features with Allen *et al.* (1995) but differs fundamentally from theirs in that an orthogonal coordinate system rather than a sigma coordinate system is used and surface cooling is imposed as the upper boundary condition. The surface thermal condition is the same as that in Akimoto *et al.* (1990). In Table 1, main features of numerical model are compared to other previous models which are of direct relevance to this study. Unlike the hydrostatic model, the nonhydrostatic model resolves directly the vertical motion that is important (unimportant, respectively) for the small-scale (large-scale, respectively) coastal circulation (see Akimoto, 1990; Chao, 1992). As a consequence, the nonhydrostaticity in a model is particularly important when the surface cooling is imposed because it induces the vertical motion due to the hysrostatic instability near the surface.

In section 2, model and boundary condition are presented. In section 3, the coastal circulations for various situation are investigated. Finally, discussion and summary is given in section 4.

MODEL BOUNDARY AND INITIAL CONDITIONS

As in Cheong and Han (1997), the cylindrical coordinate system is used to calculate two dimensional cross-shelf circulation in a vertical section with constant bottom-slope. Cylindrical coordinate system has an advantage over the sigma-coordinate system that the cylindrical coordinate system is an orthogonal coordinate system. Model geometry of

Table 1. Comparison of two-dimensional numerical models used for the coastal seawater circulation

model	bottom slope	wind stress	thermal condition at the surface	hydro-staticity
Akimoto *et al.* (1990)	not considered	not considered	cooling	non-hydrostatic
Feliks (1991)	not considered	considered	cooling	hydrostatic
Allen and Newberger (1996)	considered	considered	heating	hydrostatic
This study	considered	considered	cooling	non-hydrostatic

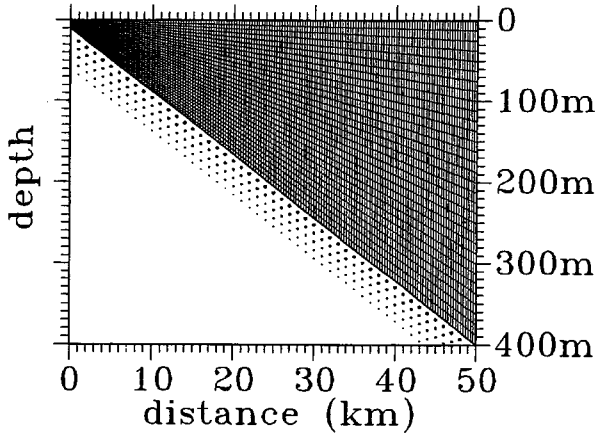

Fig. 1. Geometry of the model for bottom slope of 0.45° and grid boxes for numerical simulation.

slab-symmetry is shown in Fig. 1. The model domain consists of two radial and two arcs of circles with the same center. The inner arc at $r=r_0$ corresponds to the coast and the outer one to the offshore boundary. Details are refered to Cheong and Han (1997).

Governing equations used are basically the same as in Cheong and Han (1997) with exceptions that the alongshore momentum equation is included and the rotation effect is considered in the present study. By eliminating the pressure terms, the momentum equations of r and θ direction are combined into the vorticity equation with the use of continuity equation. The basic equations are written as follows.

$$\frac{d\zeta}{dt}=\frac{g}{\rho_0}\left\{-\cos\theta\frac{\partial}{r\partial r}(\rho r)+\frac{\partial}{r\partial\theta}(\rho\sin\theta)\right\}+\sin\theta\frac{\partial}{r\partial r}(fvr)-\frac{\partial}{r\partial\theta}(fv\cos\theta)+\frac{1}{r}\left(A_H\frac{\partial}{\partial r}r\frac{\partial}{\partial r}+A_V\frac{1}{r}\frac{\partial}{\partial\theta^2}\right)\zeta \quad (1)$$

$$\frac{d\rho}{dt}=+\frac{1}{r}\left(K_H\frac{\partial}{\partial r}r\frac{\partial}{\partial r}+K_V\frac{1}{r}\frac{\partial}{\partial\theta^2}\right)\rho \quad (2)$$

$$\frac{dv}{dt}=-f(u\cos\theta+w\sin\theta)+\frac{1}{r}\left(A_H\frac{\partial}{\partial r}r\frac{\partial}{\partial r}+A_V\frac{1}{r}\frac{\partial}{\partial\theta^2}\right)v \quad (3)$$

where

$$\frac{d}{dt}\equiv\frac{\partial}{\partial t}+\frac{1}{r}\left\{ru\frac{\partial}{\partial r}+w\frac{\partial}{\partial\theta}\right\} \quad (4)$$

$$\zeta=\frac{1}{r}\left\{\frac{\partial}{\partial r}(rw)-\frac{\partial u}{\partial\theta}\right\} \quad (5)$$

and A_H and A_V are eddy viscosity, K_H and K_V eddy diffusivity of r and θ direction, respectively. u and w represent the velocity components in the r and θ directions, respectively. θ increases upward and set to be θ=0 at the upper boundary. ρ_0(ρ, respectively) is the reference (perturbed-density, respectively) and v is the alongshore flow of which positive direction is oriented out of the page. g is the gravitational acceleration (=980 cm/s²) and the Coriolis parameter is given $f=8\times10^{-5}$ for all experiments. Velocities and vorticity are expressed in terms of the streamfunction as follows:

$$u=-\frac{\partial\psi}{r\partial\theta} \quad (6)$$

$$w=\frac{\partial\psi}{\partial r} \quad (7)$$

$$\zeta=\nabla^2\psi=\frac{1}{r}\frac{\partial}{\partial r}r\frac{\partial}{\partial r}\psi+\frac{1}{r^2}\frac{\partial^2}{\partial\theta^2}\psi \quad (8)$$

Though the bottom slope in the East Sea is not constant, it is nearly constant within several tens kilometers from the coast. The bottom slope is set to be 0.45 degree, which is the typical slope of the continental shelf near the coast of the East Sea. If not stated otherwisely, the numerical domain is determined so that the depth at the coast and the offshore boundary is 10 m and 400 m, and the horizontal distance is L=50 km, when the bottom slope (s) is 0.45 degree. Hereafter, the offshore distance ($r\cos\theta$-r_0) is denoted as x and the depth ($r\sin\theta$) is as z.

The boundary conditions are

$$\text{at } x=0,\ u=\frac{\partial v}{\partial x}=\frac{\partial\rho}{\partial x}=\frac{\partial w}{\partial x}=0, \quad (9a, b, c, d)$$

$$\text{at } x=L,\ u=\frac{\partial v}{\partial x}=\frac{\partial\rho}{\partial x}=\frac{\partial w}{\partial x}=0, \quad (10a, b, c, d)$$

$$\text{at } z=0,\ A_V\frac{\partial u}{\partial z}=\tau_u,\ A_V\frac{\partial v}{\partial z}=\tau_v,\ K_V\frac{\partial\rho}{\partial z}=Q, \quad (11a, b, c)$$

$$\text{at the bottom, } u=v=w=\frac{\partial\rho}{\partial z}=0, \quad (12a, b, c, d)$$

where τ_u and τ_v denote the surface wind stress of u and v components and Q represents the buoyancy flux that should be calculated from the surface heat flux. In Eq. (11) we assumed that the eddy viscosity and diffusivity of z-direction (x-direction) are the

same as those of θ-direction (r-direction) because θ is very small within the model domain.

In a model using the Boussinesq fluid, for which the density perturbation is written as $-\alpha T$ with $\alpha(\approx 1.43\times10^{-4}$g cm$^{-3}K^{-1}$ at 10°C and salinity of 35‰) and T being the volume expansion coefficient and temperature perturbation, respectively, the buoyancy flux (Q) is related to the heat flux (q_h) in the form $Q=10^3\alpha(\rho_s c_p)^{-1} q_h$, where $\rho_s(\approx 1$ g cm$^{-3})$ and $c_p(=4.3\times10^7$ erg g^{-1} K^{-1} at 10°C) are the average density and the specific heat for constant pressure of the seawater, respectively. The wind stress and surface cooling over the East Sea vary time to time and increase during cold-air outbreaks. In this study, representative values of $\tau\equiv(\tau_u^2+\tau_v^2)^{1/2}=2.5$ dyne/cm^2 $\equiv\tau_0$ for wind stress and 300 W/m^2 for surface cooling rate are used. Neglecting few percents error that may come from the variation of the physical properties such as α, ρ_s and c_p with the temperature or salinity, then, we have $Q=10^{-6}$ g cm^{-2} s^{-1}. Considering the observational analysis (Kang *et al.*, 1994), the orientation of the wind stress vector q=arctan (τ_u/τ_v), i.e., the angle measured from the alongshore axis (directed out of the paper) is given to vary 0 to 60 degrees. The eddy coefficients of viscosity and diffusion are $A_H=K_H=4\times10^4$ cm^2 s^{-1}, $A_V=K_V=10$ cm^2 s^{-1}.

Equations (1), (2), and (3) are time integrated by approximating them to the finite difference form with the initial condition of no motion. To get an initial density profile in the model, we ploted the profile of σ_t[1)] observed at three stations (03, 04 and 05) of the serial line 107 located at (38° 12'6"N, 128°50'6"E), (38°12'6"N, 129°03'5"E) and (38°12'6" N, 129°22'3"E), respectively, released by National Fisheries Research and Development Agency (NFRDA). The observation is carried out once a month. In the left panel of Fig. 2 we show the total 33 vertical profiles of σ_t observed in December from 1982 tp 1995 excluding 1988, 1991 and 1992. The profile differs from observation to observation showing a cosiderable amplitude of fluctuation in the upper layer of 100 m depth. Reflecting the observed features qualitatively, we adopt an idealized density profile as an initial condition. The right

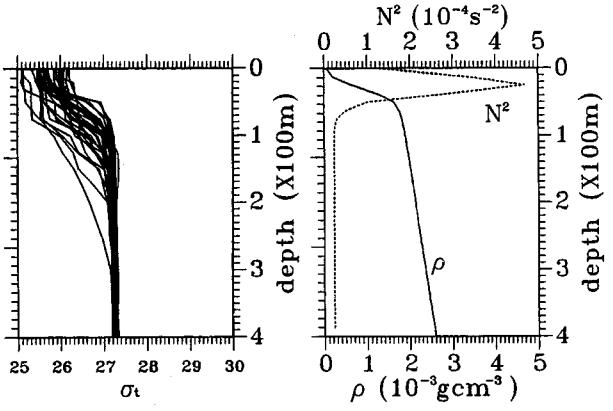

Fig. 2. (Left) The observed σ_t at a serial line 107. For details see the text. (Right) Initial density profile (solid line) and squared buoyancy frequency.

panel of Fig. 2 shows the initial density $\bar{\rho}(z)$ and squared buoyancy frequency $N^2(z)=\frac{g}{\rho_0}\frac{d\bar{\rho}}{dz}$, which are horizontally uniform. One significant difference of the model and observed density structure is that the former exhibits a constant gradient below 100 m depth while the latter is nearly constant there.

The whole domain is divided into grid space of 160 and 32 in radial and azimuthal directions, respectively. The horizontal scale of one grid is 312. 5 m, and the vertical scale of one grid at the coast and the offshore boundary are 0.3125 m and 12.5 m, respectively. One time step of the numerical integration, Δt, is 36 seconds. The centered scheme for time and space differenciation is used. For every time step, the streamfunction is obtained from the finite difference form of Eq. (8) and the procedure is refered to Cheong and Han (1997). Velocities are obtained from the relation of Equations (6) and (7).

It is known that a cold-air outbreak in general lasts for about a week (Chao, 1992; Lim, 1995), during which the strength and orientation of the surface wind are maintained nearly constant. In this study, however, we assume that the surface condition corresponding to a cold-air outbreak continues to exist in order to see a longer time response of the coastal sea. The wind stress, then, is given to be independent of horizontal distance and set to increase exponentially from 0 to τ_0 for two days to ensure the stability of the numerical integration as was done by Allen *et al.* (1995). The surface cooling is introduced in a similar way. It is independent of x and increases from 0 to Q for two days.

The standard experiment is one where q=30°, s=0. 45° and Q=0.

[1)] In the Boussinesq model, the density (ρ), which represents the buoyancy effect, should be replaced by the potential density (σ_θ) rather than σ_t of the seawater. However, in the upper layer of about 1000 m-depth the difference between the observed values of σ_t and σ_θ is less than 0.01.

RESULTS

Standard experiment

Fig. 3 shows the distribution of the perturbed density (ρ), streamfunction (ϕ), and alongshore flow (v) at day 6, 12, and 18, respectively, for the standard experiment. Since our main concern is the response in the area near the coast, we do not present the field of variables offshore of 38 Km where the boundary effect is dominant. Since a steady wind forcing is applied and steady thermal forcing as can maintain the initial stratification does not exist, the flow field will continue to evolve slowly. It is seen (Fig. 3) that the density stratification becomes weaker with time. A well-mixed surface layer develops, which is, on average, about 20 m deep by day 18 and deepens toward the coast. A density front, which separates the vertically almost uniform density field of the nearshore from the strongly stratified density field of the offshore region, appears from the early stage and continues to move offshore with time, reaching 10 km offshore distance by day 18. From the cross-shelf circulation pattern, in which the upper layer the flow directs onshore, it can be stated that the wind stress used in the standard experiment (q=30 degrees) favors a downwelling circulation. Note that in the upper layer near the coast an inversely stratified density field is observed, which is a model point that is different from the results of downwelling experiment done by Allen and Newberger (1996) under the condition of a surface heating. This will be removed by surface heating because it tends to make a stable stratification near the surface.

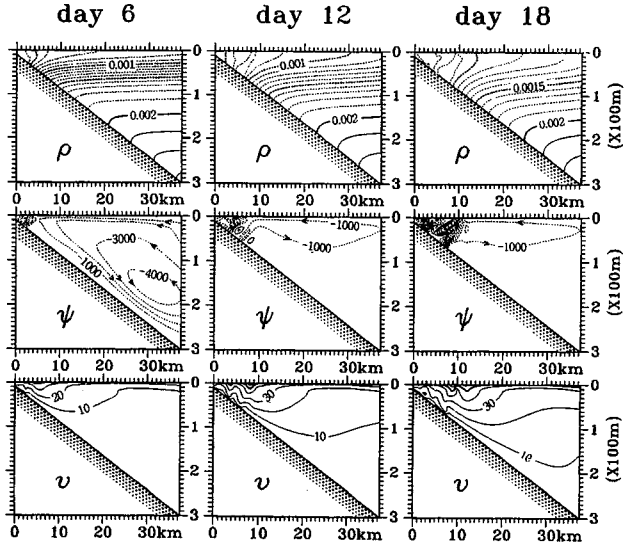

Fig. 3. Distribution of the perturbed density (ρ), streamfunction (ψ), and alongshore velocity (v) at day 6, 12, and 18, respectively in case of the standard experiment. Contour intervals are $\delta\rho$=0.0001 gcm^{-3}, $\delta\psi$=1000 cm^2 s^{-1}, and δv=10 cm s^{-1}. Values lower than 0.002 are in dashed lines for density field and negative (positive) values are in dashed (solid) lines for the streamfunction and alongshore velocity. Thick lines are used every 5 contour intervals.

By day 6, the cross-shelf circulation that extends well to the bottom in the whole domain is composed of two circulation cells of positive vorticity ($\zeta > 0$) and one negative vorticity cell (not indicated in this figure because of large value of contour interval). One of them is a huge cell that occupies almost the whole section except an inshore region of typically 5 km-width, which is responsible for the formation of bottom mixed layer. The circulation pattern changes significantly after day 6: The vertical extent of the huge cell is decreased and the circulation cells are strengthened in the inshore region of the density front so that the onshore velocity reaches several cm s^{-1} by day 18. The cross-shelf circulations are confined to the upper layer of about 50 m or so which corresponds to the mixed layer.

The nearshore circulation cells share several common features with the results of Allen and Newberger (see the 3rd column of Fig. 15 in their paper) inspite of differences in surface thermal boundary condition, hydrostaticity, and other parameters of the models. Firstly, the axis of the cell is perpendicular to the bottom slope and nearly parallel to the isopycnals near the bottom. Secondly, the cell extends from the bottom to the top. Thirdly, the horizontal size is about 2 km which is larger than the vertical size by more than one order.

The oscillation of the streamfunction at the bottom did not appear in the offshore region of the density front, which is caused by the fact that the cross-shelf circulation exists far away the bottom. Unlike the results of Allen and Newberger (1996), in which the density in the inshore region of the density front is homogeneous even in the presence of strong small-scale circulations, the vertical density structure in our experiment shows an irregular variation due to an intense cross-shelf motion.

The alongshore flow, which is everywhere positive (i.e., out of the paper) and one order larger than the cross-shelf flows, increases upward and with time. It shows fluctuations near the bottom due to the cross-shelf circulations. The greatest alongshore flow is formed over the density front, which reaches

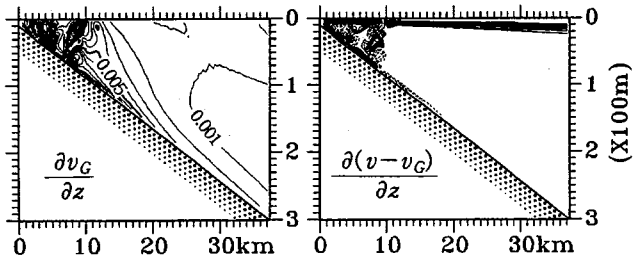

Fig. 4. The vertical differentiation of v_G (left panel) and the v-v_G (right panel), where v_G and v are the alongshore geostrophic flow and alongshore flow, respectively. The contour interval is 0.001 s^{-1} and every 5 contours thick lines are used.

a value larger than 50 ms^{-1} by day 18. A great portion of the strong alongshore flow could be explained by the thermal wind balance

$$\frac{\partial v_G}{\partial z} = -\frac{g}{f\rho_0}\frac{\partial \rho}{\partial x} \tag{13}$$

where v_G is the alongshore geostrophic current. In Fig. 4, the vertical differentiation of the alongshore geostrophic flow (v_G) is presented also with that of the difference between v_G and alongshore flow. In the offshore region of the density front the thermal wind balance (or geostrophic balance) holds to a good approximation except the upper boundary, while it is not the case in the inshore region of the density front. This is a consequence of strong vertical circulation, i.e., nonhydrostatic motion.

Sensitivity to the orientation of the wind-stress vector

The orientation of the wind stress vector caused by the cold-air outbreak varies from case to case (Lim, 1995). It is in general, as can be expected from Na (1988) and Kang *et al.* (1994), the northwesterly because the cold-air originates in the Eurasian continent. In this section we investigate the response sensitivity of the coastal circulation to the orientation of the wind stress vector when the magnitude of the wind stress vector is fixed.

Fig. 5 shows the fields of density, streamfunction, and alongshore flow when the offshore angle of the wind-stress vector q is given 0, 45, and 60 degrees, respectively. As q increases, the cross-shelf circulation becomes weak, and as a result the position of the density front appears to be closer to the coast. This is a direct consequence of the strong offshore-component of the wind-stress. This can be explained easily if we remember that the net transport of

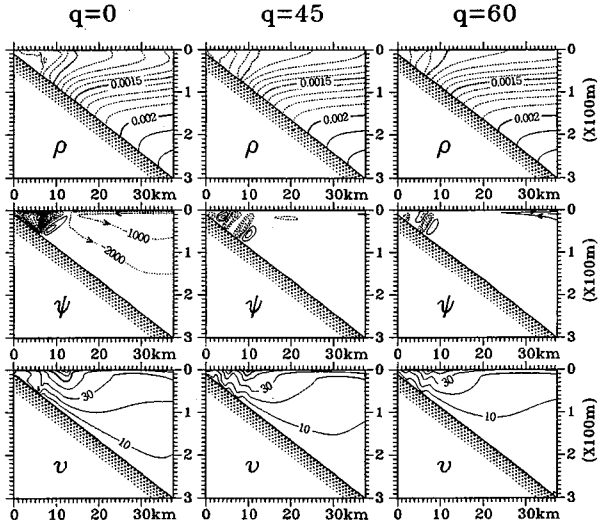

Fig. 5. Distribution of the perturbed density (ρ), streamfunction (ψ), and alongshore velocity (v) at day 18 for the affshore angle (q) of the wind-stress of 0, 45, and 60 degrees, respectively. Refer to Fig. 3 for contour intervals and units.

mass in the upper Ekman layer is in the direction rotated 45 degrees clockwise from the surface wind-stress vector.

For q=0, the cross-shelf circulation is so strong that an upper-layer inversion can take place within 30 m depth. In Allen and Newberger (1996), such an inversion does not occur because the surface heating works as a stabilizing effect. For offshore angle of 60 degrees, a reversed cross-shelf circulation tends to develop in the offshore region. The fields of the alongshore flow are qualitatively similar to one another and correspondingly less sensitive to the q factor. Among the four experiments including the standard experiment, the number of small-scale circulation cells are largest when q=45 degrees.

To see the behavior of the small-scale circulation cells at the bottom layer, we present in Fig. 6 the time variation of azimuthal velocity at the 4 grid away from the bottom for various orientation of the wind-stress vector (q). When the wind-stress vector is set to be parallel to the alongshore direction, the small-scale circulation cells propagate offshore with a constant speed of 0.3 km/day. In early stage, the small-scale circulation cells show onshore propagation in case of q=30 degrees (i.e., the standard experiment) with a comparable speed to the case of q=0, but after day 13 they behave rather irregularly. In cases of q=45 and 60 degrees, the cells exhibit a regular propagation toward the coast, which are

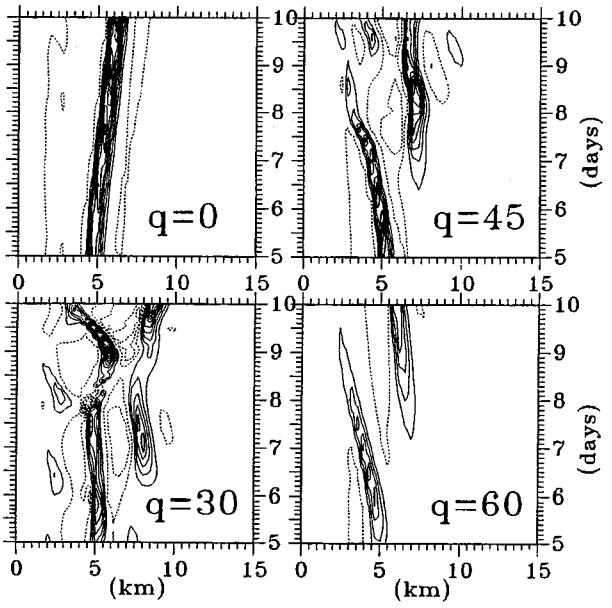

Fig. 6. Time variation of the azimuthal velocity (w) at the 3.5 grids away from the bottom for various offshore angle (q) of wind-stress vector. Contour interval is 0.006 cm s^{-1} and negative values are in dashed lines.

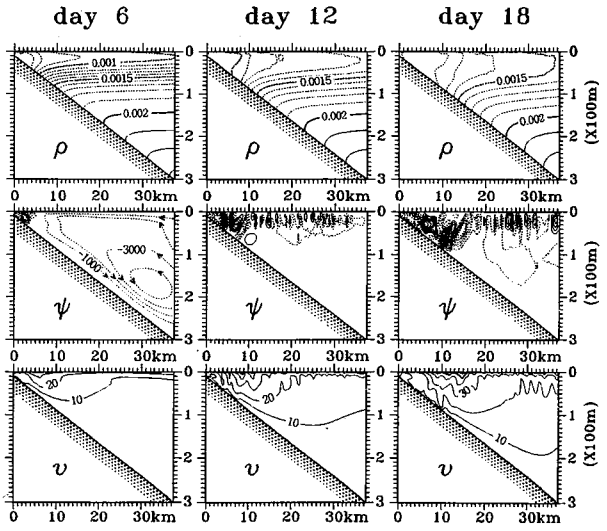

Fig. 7. The same as Fig. 3 except that a constant surface-cooling is imposed at the surface.

seen to be generated near the density front. For q=60 degrees the onshore propagation speed is about 0.5 km/day, that is nearly twice of the offshore propagation speed for the q=0 case but is much smaller than that of Allen and Newberger (1996).

Effect of the surface cooling

The surface heating plays a role as a stabilizing factor in the upper layer by compensating the high-density advection accompanying the cross-shelf circulation. If the surface heating is replaced by the surface cooling, the density stratification in the upper layer is easily destabilized by the combined effect of cooling and advection. In this section, the effect of the surface cooling is investigated by imposing a constant heat-flux condition at the surface in the standard experiment. Q=10^{-6} is given in Eq. 11c. Two days after the initiation of the surface cooling, we added infenitesimal perturbation in density field to trigger the vertical convective motion.

The results are shown in Fig. 7. By day 6, the fields of variables are almost identical to those for the standard experiment except the the upper layer of the density field, where an unstable density structure is established within depth of about 10-20 m. A noticeable change in the upper layer is found by day 12: Small-scale cells of convective motions, confined to the upper layer, appear in the offshore region, of which horizontal scale is typically 2 km. Recirculation cells near the coast remain almost unchanged compared to the standard experiment. The gross feature of the alongshore flow is not modified by the convective cells though the fluctuations with small scale are present.

By day 18, the size of convective cells increased slightly in the both directions. In the offshore region, the density structure is divided into four layers from the surface; the unstable, neutral (mixed), stable and mixed bottom layers. As the surface cooling continues to exist, the thickness of the mixed layer increases while that of the surface unstable layer, which is about 10~20 m, remains little changed. It is of interest to note that the small-scale circulation cell nearest to the density front coalesced with the convective cell and the small-scale circulation cells are slightly distorted by the surface cooling.

Presented in Fig. 8 is the time variation of the the stream function ψ at the third grid from the surface. From day 10, the convection cells begin to develop only at two locations of which distance is about 10 km, and new cells are generated successively in the offshore side. The typical lifetime of the cells are 5~8 hours. However, by day 12 the lifetime of the cells increases appreciably, which means vertical growth of the cells. It is worthy to note that the convection cells do not propagate horizontally in spite of the cross-shelf circulation.

Experiment without the wind-stress (shown in

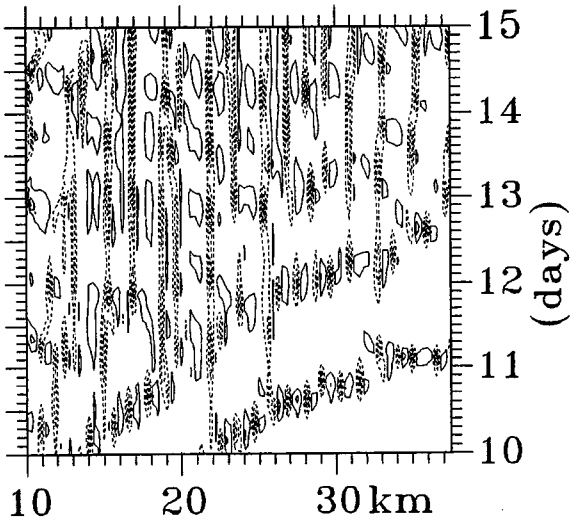

Fig. 8. Time variation of the stream function ψ at the 2.5 grids away from surface. Contour interval is δψ=1000 $cm^2 s^{-1}$, and negative values are in dashed lines.

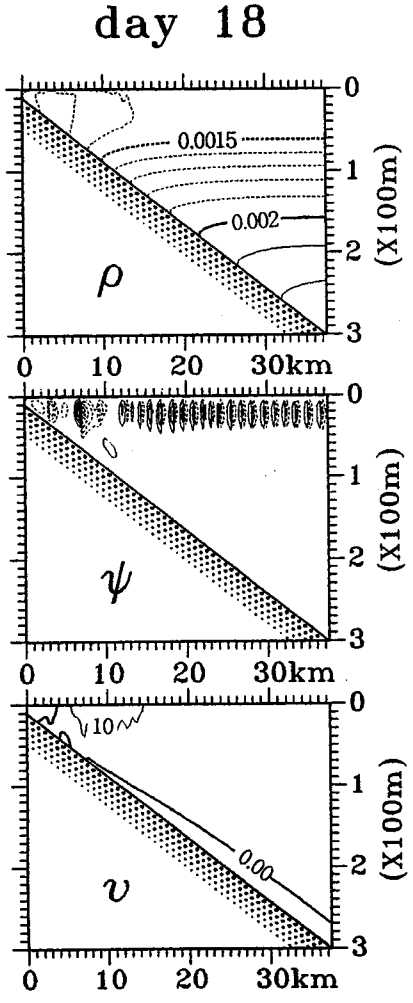

Fig. 9. Distribution of the perturbed density (ρ), stream function (ψ), and alongshore velocity (v) at day 18 for the experiment where the wind-stress forcing is removed from the experiment of Fig. 8.

Fig. 9) revealed that the vertical extent of the convective motion due to surface cooling was significantly reduced, and at the same time the horizontal scale of them was also decreased. Note that a density front is formed near the coast even without the downwelling circulation. Inshore of the density front, a well-mixed homogeneous layer exists. The isopycnals near the bottom are more horizontally aligned than in the experiment with the downwelling favorable wind-stress forcing. Our result suggests that a shallow sea front is can be established even without the lateral buoyancy flux if the bottom slope exists (cf. Akimoto *et al.* 1990). A positive alongshore current, which is much smaller compared to the previous experiments such as in Fig. 8, is also found in this experiment. The time evolution and formation process of this alongshore current will be persued more in detail in a separate paper.

Effects of the bottom slope

The bottom slope in the coastal sea varies from place to place. To see the effect of the bottom slope on the coastal circulation, we carried out further two experiments in which the bottom slope is doubled or reduced by half. The initial density structure for the half slope case is given the same as that of the standard case. In case of double slope, the density at offshore distance where the depth is greater than 400 m is given as to have the same N^2 as that of levels just above 400 m.

Fig. 10 compares the field variables for different bottom slope. The upper (lower) figures are those for bottom slope of 0.225 (0.9) degrees. For smaller bottom slope, the density front is formed far away

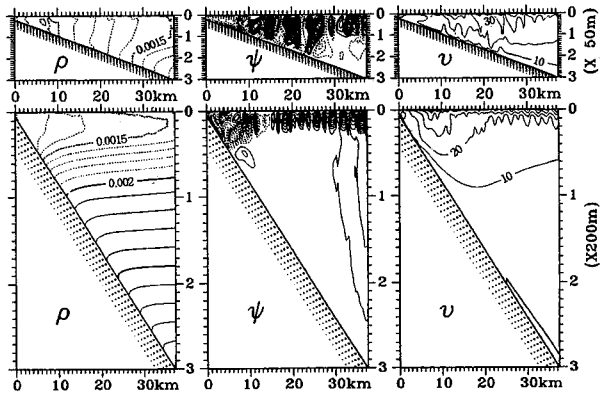

Fig. 10. Distribution of the perturbed density (ρ), stream function (ψ), and alongshore velocity (v) at day 18 for the small bottom-slope (upper row) and doubled bottom-slope (lower row).

from the coast, and the mixed layer broadens horizontally accompanying much more small-scale circulation cells compared to the standard experiment. Note that the small-scale circulation cells are not aligned in the direction perpendicular to the bottom, but they are rather vertically (z-direction) aligned. As can be seen from the streamfunction field, the fluid depth is small enough to allow the convective motions to reach the bottom. As a result, in the inshore region of nearly 30 km the seawater is vertically well mixed and the density increases almost linearly with the horizontal distance. For the increased bottom slope, the main features are very similar to those of the standard case in a qualitative sense.

When the wind stress is strong, whether the density decreases or increases with horizontal distance in the regions near the coast is determined by the direction of the wind stress. For example, under the upwelling favorable wind stress condition (e.g., see Fig. 1 of Federiuk and Allen, 1996), the density decreases with the offshore distance increases. As we have seen in Fig. 9, however, the horizontal density variation can be established even when the wind stress is absent and horizontally uniform surface cooling is imposed (Not shown here, we found, through an experiment which is the same as that shown in Fig. 9 except that the surface heating is applied, such a density structure is not produced). It means that the convective cells over a sloping bottom, on which the buoyancy flux does not exist, can give rise to a large circulation cell whose strength is one order smaller than the individual convective cell.

DISCUSSION AND SUMMARY

Two-dimensional cross-shelf circulations were investigated using Boussinesq fluid under the surface condition of the wind-stress and/or surface cooling in the presence of the bottom slope, with idealized conditions of surface forcings and geometry that are of typical ones found in the East Sea (around the 107 serial line). Numerical model used in this study shares some common features with that used by Allen and Newberger (1996), but an important difference exists that our model incorporates the surface cooling and nonhydrostatic process, and uses the cylindrical coordinate system as in Cheong and Han (1997). For the vertical turbulent kinetic viscosity and diffusivity we used a constant value because, as indicated by Allen and Newberger (1996), the basic qualitative flow features are not modified by a particular parametrization method for these. The constancy of these parameters, however, does have an undesirable effect that it weakens the strong stratification of density field in the vicinity of the pycnocline, while it does not for the case of parametrized viscosity and diffusivity because they are evaluated to be small in the region where the static stability is large. Therefore, in the upper layer where the unstable stratification is maintained due to surface cooling the effect of viscosity and diffusion might have been underestimated. The standard parameter for the offshore angle is kept 30 degrees, based on the observational facts (Na, 1988; Kang *et al.*, 1994).

When the surface cooling is absent a well mixed-layer develops just above the pycnocline due to a strong onshore flow. Not shown here, under the upwelling-favorable wind-stress condition (for the angle larger than 90 degrees), such a mixed layer less easily develops. For a wide range of offshore angle of the wind-stress vector, small-scale circulation cells, which are aligned in the direction perpendicular to the bottom, are formed near the coast with a horizontal scale of about 1~2 km and propagate onshore with a speed of 0.3 km/day.

If the surface cooling is incorporated the flow characteristics are greatly changed. The surface cooling produces gravitational convection in the surface layer, which enhances the development of the mixed layer. The vertical structure of the density in the offshore region is divided into four layers: The unstable layer near the surface which is directly cooled by the surface heat-flux, the homogeneous mixed-layer generated by combined effect of the gravitational convection and horizontal density advection, stable and mixed bottom layer. The coastal density-front moves offshore compared to the experiment without the surface cooling. The effect of the surface cooling begins to appear at least 6 days after initiation of cooling for the standard experiment, which will be changed if the parameters such as cooling rate is given a different value.

Experiment without the wind-stress forcing showed that the coastal front (density front) can be formed by the effects of bottom slope and surface cooling. That is, the lateral buoyancy flux which was considered as a major factor in producing a shallow sea front in the model of contant depth (e.g.,

Akimoto *et al.* 1990) is not essential for the formation of the density front if the bottom slope exists as in the present model. For a smaller (larger) bottom slope, the density front moves far offshore (onshore) if other parameters are fixed, because the onshore volume transport remains almost constant.

Comparison of Fig. 7 and 9 in which the wind stress is incorporated and excluded, respectively, indicates that the wind stress is ultimately responsible for the formation of the bottom mixed layer. The mechanical forcing due to the wind stress drives a huge circulation cell occupying the whole domain, which makes a downward motion along the bottom and finally a mixed layer is formed.

Of particular importance of the bottom slope for the coastal circulation in case of surface cooling was found to generate a large circulation cell. In the procedure lying on the coalescence process of convective cells, the Coriolis force presumably plays an important role as can be imagined from the strong alongshore current formed just over the density front (see Fig. 9). The effect of the bottom slope on homogenizing the vertical density increases as the slope (Fig. 10). This fact is easily understood if one thinks of a rectangular cross section near the coast with a great depth, i.e., the slope angle of 90 degrees. In such case, there is no reason that the boundary effect of surface cooling on the circulation is concentrated near the coast if the wind stress is absent.

The structure of the coastal circulations in the East Sea is not 2-dimensional, i.e., the alongshore variation of the density and velocities is very large. Further, the initial condition and parameters used are somewhat idealized ones, while the observed surface condition varies time to time and has a considerable variation in the offshore direction. Therefore, the application of the results of this study is limited to the averaged feature in the alongshore direction. Nevertheless, some results of the present study have application to the prediction of the response of the coastal sea if the time-scale of three dimensional variability is long enough.

Three-dimensional features of the sea water circulations near the coast driven by surface cooling and wind-stress will be persued in the future.

ACKNOWLEDGEMENTS

The valuable comments of referees are greatly appreciated. This study was supported by Korean Ministry of Education through research fund in 1996.

REFERENCES

Akimoto, K., N. Imasato and T. Awaji, 1990. A numerical study of a shallow sea front generated by buoyancy flux: Generation mechanism. *J. Phys. Oceanogr.*, **20**: 172-189.

Allen, J.S. and P.A. Newberger, 1996. Downwelling circulation on the Oregon continental shelf. Part I: Response to idealized forcing. *J. Phys. Oceanogr.*, **26**: 2011-2035.

Allen, J.S., P.A. Newberger and J. Federiuk, 1995. Upwelling circulation on the Oregon continental shelf. Part I: Response to idealized forcing. *J. Phys. Oceanogr.*, **25**: 1843-1866.

Chao, S.-Y., 1992. An air-sea interaction model for cold-air outbreaks. *J. Phys. Oceanogr.*, **22**: 821-842.

Cheong, H.-B. and Y.-H. Han, 1997. Numerical study of two-dimensional gravity currents on a slope. *J. Oceanogr.*, **53**: 179-192.

Federiuk, J. and J.S. Allen, 1995. Upwelling circulation on the Oregon continental shelf. Part II: Simulations and comparisons with observations. *J. Phys. Oceanogr.*, **25**: 1867-1889.

Federiuk, J. and J.S. Allen, 1996. Model studies of near inertial waves in flow over the Oregon continental shelf. *J. Phys. Oceanogr.*, **26**: 2053-2075.

Feliks, Y., 1991. Downwelling along the northeastern coasts of the eastern Mediterranean. *J. Phys. Oceanogr.*, **21**: 511-526.

Kang, I.-S., M.-K. Kim and T.-B. Shim, 1994. Seasonal variation of surface heat budget and wind stress over the seas around the Korean Peninsula. *J. Korean Soc. Oceanogr.*, **29**: 325-337.

Kim, Y.-S. and R. Kimura, 1995. Error evaluation of the bulk aerodynamic method for estimating heat flux over the sea. *J. Korean Meteor. Soc.*, **31**: 399-413.

Lim, G.-H, 1995. Spatial and temporal evolution of the tropospheric upper and lower level winds during the cold surge periods in the East Asia. *J. Korean Meteor. Soc.*, **31**: 373-392.

Na, J.-Y., 1988. Wind stress distribution and its application to the upper-layer structure in the East Sea of Korea. *J. Oceanol. Soc. Korea*, **23**: 97-109.